Superconducting Quantum Interference Device (SQUID)

Aaron Kraft, Christoph Rupprecht, Yau-Chuen Yam

***Abstract*—The superconducting state, a macroscopic quantum phenomena which exhibits resistanceless electric transport, enables many unique measurements and experiments. One application is a Superconducting Quantum Interference Device (SQUID), which can measure magnetic flux with incredible precision. Based on the Josephson Effect, SQUIDs have become instrumental in Condensed Matter Physics for their precision and versatility.**

I. Introduction

Josephson first formulated the theory for tunneling between superconductors in 1962. His result, for which he won the Nobel prize in 1972, indicated that a tunneling supercurrent would occur between two superconductors separated by a small insulating junction. According to his calculations this supercurrent would be related to the phase difference between the two superconductors. In practice this principle enables the phase difference of two superconducting materials to be measured. And since the phase of a quantum state is also altered by magnetic flux, this magnetic flux can be measured precisely. Since its first construction in 1964, SQUIDs have become an instrumental part of condensed matter physics. Used most frequently as a highly precise magnetometer, SQUIDs can also be adapted and applied to other problems and combined with novel techniques. In this paper we will derive the equations that govern the behavior of a SQUID, and give a brief overview of its many interesting applications.

II. Physics of a SQUID

A Josephson Junction, as shown in Fig. 1 forms the foundation of a SQUID. There are two types of SQUIDs commonly used in applications: a DC SQUID, which contains two parallel junctions, and an RF SQUID, which contains just one junction. To begin our treatment of SQUIDs we will therefore turn to the dynamics of a Josephson Junction. We will then look into the effects of an external magnetic field on a Josephson Junction in order to show how a SQUID can measure magnetic flux.

A. The Josephson Junction

As shown in Fig. 1, a Josephson junction consists of two superconductors separated by an insulating material. Interesting physics arises due to the tunneling of cooper pairs across the insulating barrier. While this is quantum mechanical in nature, we do not need to turn to BCS theory in order to understand this. Instead we can choose a phenomenological and macroscopic ansatz for the superconductors wave function, which is explained in more detail in reference [5] as well as the Appendix:

$$\Psi(\vec{r}) = \sqrt{n_s} \cdot e^{i\phi(\vec{r})} \tag{1}$$

Here $n_s = \Psi \cdot \Psi^*$ is the cooper pair density and $\phi(\vec{r})$ is the phase. This wave function in and of itself is very interesting and gives a clear example of how superconductivity leads to quantum behavior on a macroscopic scale. Here the wave function describes a large number of cooper pairs which are phase coherent, so we can see a quantum mechanical behavior on a classical length scale.

Therefore we can assume that the two superconductors in Fig. 1 have wave functions $\Psi(\vec{r}) = \sqrt{n_1} \cdot e^{i\phi_1(\vec{r})}$ and $\Psi(\vec{r}) = \sqrt{n_2} \cdot e^{i\phi_2(\vec{r})}$. Given that the typical width of the insulator is around 100nm, we can also assume that the two superconductors are weakly coupled with a coupling constant K, i.e. cooper pairs can tunnel between the two superconductors, but they still separate enough that they are described by different wavefunctions. The Schrodinger equation for the two superconductors ($i, j \in \{1, 2\}$ and $i \neq j$) then reads:

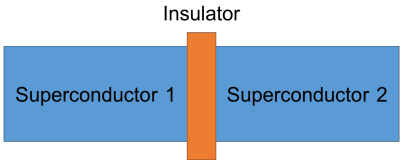

Fig. 1. **A Josephson junction**: It is made of two superconductors connected through a small insulating layer.

$$i\hbar \frac{\partial \Psi_i(\vec{r})}{\partial t} = E_i \Psi_i + K \Psi_j \tag{2}$$

Assuming that we have the same type of superconducting material on each side of the barrier (a reasonable assumption, since in practice we can design the Josephson Junction out of whatever material we choose), we know that $E_1 = E_2$. But we will also connect this Josephson Junction to a battery such that we have a potential difference $E_1 - E_2 = qV$. Choosing the reference point for energy in the middle between the energies, the Schrodinger Equation becomes:

$$i\hbar \frac{\partial \Psi_i(\vec{r})}{\partial t} = (-1)^{i+1} \frac{qV}{2} \Psi_i + K \Psi_j$$

We can now plug in our superconducting wavefunction (1) to get the following four equations for the real and imaginary parts of Ψ that describe the dynamics of tunneling cooper pairs.

$$\begin{aligned}
\frac{dn_1}{dt} &= \frac{2K}{\hbar}\sqrt{n_1 \cdot n_2} \cdot sin(\phi_2 - \phi_1) \\
\frac{dn_2}{dt} &= -\frac{2K}{\hbar}\sqrt{n_2 \cdot n_1} \cdot sin(\phi_2 - \phi_1) \\
\frac{d\phi_1}{dt} &= -\frac{K}{\hbar}\sqrt{n_2/n_1} \cdot cos(\phi_2 - \phi_1) - \frac{qV}{2\hbar} \\
\frac{d\phi_2}{dt} &= -\frac{K}{\hbar}\sqrt{n_1/n_2} \cdot cos(\phi_2 - \phi_1) + \frac{qV}{2\hbar}
\end{aligned}$$

Since the current is $I = nAq\frac{dx}{dt}$ with cross section A, charge carrier density n, and charge of the carriers q, the first two equations become:

$$I_s = I_0 \cdot sin(\phi_2 - \phi_1) \tag{3}$$

where we assumed $I_0 = \frac{2K}{\hbar} 2q\Omega$ where $n_1 = n_2 = n$, and Ω is the volume of the two superconductors. This is known as the first Josephson Equation and describes how the tunneling current will depend on the phase difference between the two superconductors. But how does the phase difference evolve in time? If we again assume $n_1 = n_2 = n$ and subtract the third and fourth equations from each other we get:

$$\frac{d}{dt}(\phi_2 - \phi_1) = \frac{qV}{\hbar} \tag{4}$$

which is the second Jospehson equation and describes the time evolution of the phase difference given an external voltage. These two Josephson equations describe the phase evolution of the two superconductors and give rise to very interesting and non-intuitive physics. Suppose for example that there is a constant voltage applied to our Josephson Junction. Then (4) tells us that the phase difference will evolve linearly in time. Plugging this back into (3), we see that we will then get an AC current. This is known as the AC Josephson effect.

But what if we apply no external voltage? The phase difference, given by (4), now becomes constant. Again plugging this back into (3) we see a constant supercurrent flowing despite no external voltage. This very unconventional behavior results directly from the phase coherence of the cooper pairs, which is also known as the DC Josephson effect.

B. The DC Squid

Now that we have the equations that describe just one Josephson junction, we can apply these to a loop with two Josephson Junctions in a magnetic field, as shown in Fig.2. We will see in this section that we can determine the flux present in the loop between the junctions with extreme precision because of the unique properties of the Josephson Junction.

We know now from basic quantum mechanics that the probability current in the electromagnetic field is given by the following equation [5]:

$$\mathbf{J} = \frac{1}{2}\left\{\Psi^* \left[\frac{\widehat{P} - q\mathbf{A}}{m}\right]\Psi + \Psi\left[\frac{\widehat{P} - q\mathbf{A}}{m}\right]^*\Psi^*\right\}$$

If we use (1) we see that this becomes:

$$\mathbf{J} = \frac{\hbar}{m}\left(\nabla\Phi - \frac{q}{\hbar}\mathbf{A}\right)n_s \tag{5}$$

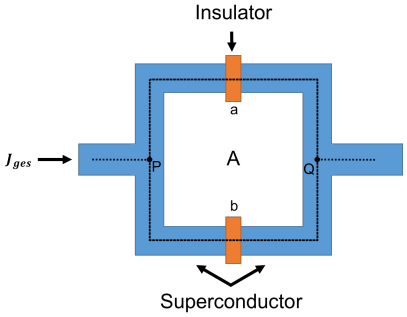

Fig. 2. **A DC SQUID** is made up two Josephson junctions a and b connected in parallel.

Since n_s is proportional to the charge carrier density of cooper pairs, we treat it as a current density.[1] Similarly, in a superconductor the current induced by an external magnetic field flows mostly on the surface, so the current density **J** will be zero at some point in the volume.

This result is shown through a detailed analysis of (5), as is done in [3]; it is closely related to the Meissner effect. Essentially, by exploiting Maxwell's equations we can obtain a differential equation for **B** using (5). By solving it we see that the magnetic field is exponentially suppressed in the superconductor. By plugging that solution into the third Maxwell equation again, this also leads to an exponentially suppressed current in the superconductor. This, in essence, is the Meissner effect, where the current on the surface creates a magnetic field which cancels the external one. Intuitively this make sense since we know that the magnetic field is not energetically favorable for a superconducting state. But for our purposes this means that there exists a path where $\mathbf{J} = 0$ around the entire loop. This allows us to simplify (5) significantly by integrating over that path from point 1 to 2 where $J = 0$.

$$\int_1^2 \nabla\phi ds = \phi_2 - \phi_1 = \frac{2q_e}{\hbar}\int_1^2 \mathbf{A}d\mathbf{s} \tag{6}$$

where q_e is the charge of the electron. Because the wavefunction is single valued, the change in the phase between the points P and Q in Fig. 2 is:

$$\phi_Q - \phi_P = \delta_a + \frac{2q_e}{\hbar}\int_P^Q \mathbf{A}d\mathbf{s} = \delta_b + \frac{2q_e}{\hbar}\int_P^Q \mathbf{A}d\mathbf{s}$$

where δ_a and δ_b are the additional phase differences of the superconductors. By using Stokes theorem we get:

$$\delta_b - \delta_a = \frac{2q_e}{\hbar}\oint \mathbf{A}d\mathbf{s} = \frac{2q_e}{\hbar}\int \mathbf{B}d\mathbf{A} = \frac{2q_e}{\hbar}\Phi$$

Another common approach that considers the gauge invariant phase change can be found in [4] and also reaches the same conclusion. The current I_{ges} is now the sum of the two branches. If we use this, the first Josephson equation with $\delta = \phi_2 - \phi_1$, $\delta_a = \delta_0 + \frac{q_e}{\hbar}\Phi$ and $\delta_b = \delta_0 - \frac{q_e}{\hbar}\Phi$ we get:

$$I_{ges} = I_0\left\{sin\left(\delta_0 + \frac{q_e}{\hbar}\Phi\right) + sin\left(\delta_0 - \frac{q_e}{\hbar}\Phi\right)\right\}$$

[1] This can be easily verified by checking the units.

We can rewrite that as:

$$I_{ges} = 2I_0 sin(\delta_0) cos\left(\frac{q_e}{\hbar}\Phi\right) \tag{7}$$

This result means that we can determine an unknown magnetic flux by measuring the current. $2I_0 sin(\delta_0)$ can first be determined by putting the dc SQUID in some known magnetic flux Φ=Φ_{known}, e.g. $\Phi_{known} = 0$ or the earth's magnetic field flux for example. Then the only independent variable would be Φ in the above equation, and we can measure the unknown magnetic flux from the current. Let's look at an concrete example to see how sensitive a dc squid can be. A typical value for the area of a SQUID used as a magnetometer is $A = 1\,cm^2$. In this case a change in the magnetic flux density of $1 \cdot 10^{-11}\,T$ is a half period in the current and can therefore be measured easily.

C. RF SQUID

As opposed to the DC SQUID, which has two junctions, the RF SQUID is composed of just one junction. In order to fully account for the behavior of the RF SQUID, we must look at the inductance of a Josephson Junction in an external field.

(C.1) One junction superconducting loop

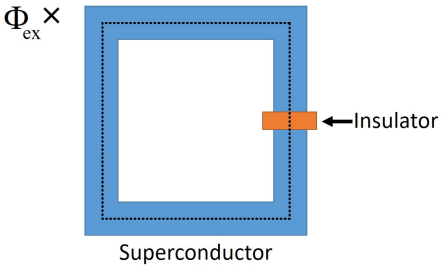

Fig. 3. A one-junction superconducting loop in an external magnetic field.

Suppose a one-junction superconducting loop is put in an external flux Φ_{ex} as shown in Fig. 3. Since in any real material, there is always a certain inductance L in a circuit we must now take that into account in our equations. By including the inductance in our equation for the flux we now find that the total flux is given by:

$$\Phi = \Phi_{ex} - LI \tag{8}$$

where I is the current flowing in the loop.

Let δ be the phase difference across the junction, then the phase change around the loop is

$$\begin{aligned}\delta + \oint \vec{\nabla}\phi d\vec{s} &= \delta + \frac{2q_e}{\hbar}\oint \vec{A} d\vec{s} \qquad (\because eq(6)) \\ &= \delta + \frac{2q_e}{\hbar}\Phi\end{aligned}$$

This phase difference must be equal to $2\pi n$ such that there is no physical observable change in our wave function. Rearranging, we get

$$\delta = 2\pi n - \frac{2q_e}{\hbar}\Phi$$

Putting this in eq(3), the current in the loop then becomes

$$\begin{aligned}I &= I_0 sin(2\pi n - \frac{2q_e}{\hbar}\Phi) \\ &= -I_0 sin(\frac{2q_e}{\hbar}\Phi)\end{aligned} \tag{9}$$

The last equality exploits the identity that $sin(2\pi n - \theta) = -sin(\theta)$. Recall from (8) that $\Phi = \Phi_{ex} - LI$. Inserting I found in (9), we find a self-consistent relation for the flux through the loop, which will be very useful in discussing the RF SQUID in (C.2):

$$\begin{aligned}\Phi &= \Phi_{ex} - LI_0 sin(\frac{2q_e}{\hbar}\Phi) \\ &= \Phi_{ex} - LI_0 sin(\frac{2\pi}{\Phi_0}\Phi)\end{aligned} \tag{10}$$

where Φ_0 is defined to be $\frac{\hbar}{2q_e}$.

(C.2) RF SQUID

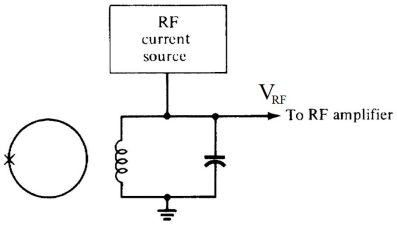

Fig. 4. Basic circuit of RF SQUID: a one-junction superconducting loop coupled to a LC circuit with a alternating current source of radio frequency.(Credits: [4])

The RF (Radio Frequency) SQUID is a one-junction SQUID loop that can be used as a magnetic field detector (Fig. 4). Although it is less sensitive than the DC SQUID, it is cheaper and easier to manufacture and is therefore more commonly used. The Quantum Design SQUID Magnetometer that is frequently used by experimenters for example, uses a one loop RF SQUID.

In the RF SQUID, the one-junction superconducting loop is coupled to a circuit driven by a RF current source, i.e. the loop would experience the flux produced by the current (Φ_{RF}). When the loop is put in some magnetic flux Φ_q that we want to measure, the total external flux is $\Phi_{ex} = \Phi_q + \Phi_{RF}$. Recall from (10) that the flux through the loop is given by $\Phi = \Phi_{ex} - LI_0 sin(\frac{2\pi}{\Phi_0}\Phi)$, which can be plotted below.

The RF SQUID has two modes of operation, the hysteretic and non-hysteretic modes. When $\frac{2\pi LI_0}{\Phi_0} > 1$, we can see from the plot of Φ vs Φ_{ex} in Fig. 5 that some parts of the curve will have positive slope and some will have negative slope. This is the 'hysteretic mode'. When the RF current and thus Φ_{RF} oscillates over time, as shown by the orange curve in Fig. 5, the Φ curve will trace out the blue of the curve. A flux quantum enters and leaves the loop during the upward and downward transitions respectively. The amount of Φ_{RF} required to conserve the energy in the transition depends on how big Φ_q is (Recall $\Phi_{ex} = \Phi_q + \Phi_{RF}$). Since the voltage in the RF circuit is related to Φ_{RF}, the voltage readout reflects the Φ_q that we are measuring. In fact, as in DC SQUID, when

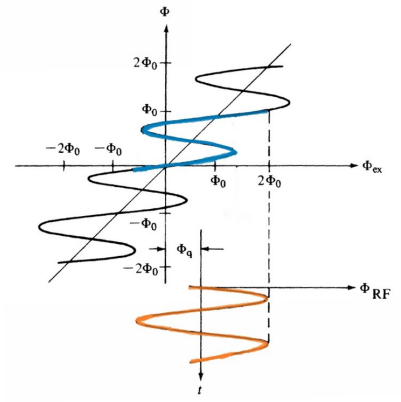

Fig. 5. Plot of Φ vs Φ_{ex} in the oscillating Φ_{RF} for $\frac{2\pi LI_0}{\Phi_0} > 1$. (Credits: [4])

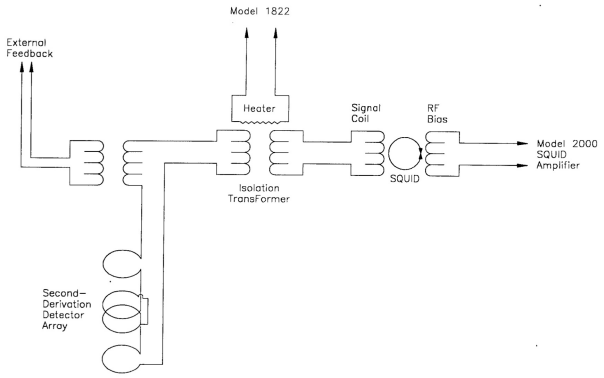

Fig. 6. A SQUID magnetometer design used in the commercial Quantum Design Magnetic Property Measurement System as shown in reference [11]. Four loops are used, two with currents going clockwise and two with currents going counterclockwise, to cancel out the effects of a static magnetic flux. The sample is moved from below the lowest loop to above the highest loop and the flux is measured as a function of position via the RF SQUID. The isolation transformer is used to decouple the SQUID loop from the pickup coils when the temperature and magnetic field are changed. Any abrupt changes in the current, like those due to changes in the external field, can damage the Josephson Junction. This design allows for the SQUID to be kept at low magnetic field and temperature while the sample temperature and field are varied.

Φ_q is changed, there is also a periodic variation of the RF voltage which is measured to determine Φ_q.

The other mode of SQUID, the nonhysteretic mode, occurs when $\frac{2\pi LI_0}{\Phi_0} < 1$, and the Φ vs Φ_{ex} relation is therefore single-valued. In this case no more energy is lost in the loop. But as Φ_q is varied, the current induced in the SQUID loop is varied. Through the mutual inductance between the SQUID loop and the RF circuit, the load on the RF circuit and thus RF voltage are similarly varied. In this way measuring the RF voltage enables us also to measure Φ_q.

III. SQUIDS IN THE REAL WORLD

Based on the principles outlined above, it is clear that SQUIDs enable the precise measurement of magnetic flux and therefore, the magnetization of crystal samples. But many issues arise in application that require more complex experimental setups than those. In practice, however, one might be interested in measuring the magnetization at temperatures and magnetic fields far above the T_c or H_c of the SQUID. Therefore designs are used that isolate the SQUID from the sample. These systems are very complex and because of this most SQUID magnetometers are not built at home but rather purchased from Quantum Design. The basic schematic of a Quantum Design SQUID magnetometer is shown in figure 6. Owing to the commercial nature of this system, the intricate details are not readily available. However the basic operation is as follows: the sample is placed in the system such that it sits inside the four pickup coils. These coils are electrically connected to a SQUID which is kept isolated from any applied magnetic field and far below T_c, usually at Liquid Helium Temperatures. The sample is then moved vertically inside the four pickup coils and the voltage across the SQUID is measured as a function of sample position. The use of four coils cancels out an externally applied magnetic field and helps to isolate the flux from the sample itself. This voltage versus position graph is then fit to a model using a complex algorithm designed by Quantum Design that uses the equations outlined above to determine the magnetization.

Data obtained via SQUID typically falls into three categories: crystal characterization, analysis of spin structure, and novel techniques that use a SQUID as part of a more complex experimental setup. Because SQUIDs are so prevalent it is difficult to give a full accounting of all the ways they are used experimentally.

The magnetization of a complex magnetic system can often be used as an order parameter, so measuring it with a SQUID is a useful way to characterize complex phase transitions. The Meissner effect in superconductors, for example, where the superconductor expels all magnetic fields below T_c, can be readily observed using a SQUID. As a superconducting sample drops below T_c, the system will react to an external magnetic field by creating its own equal and opposite field as previously outlined. In effect the superconducting system becomes magnetized so that the total internal magnetic field is zero. This change in magnetization can be used to determine the T_c of a superconducting sample with good precision. This principle is outlined in figure 7 where the the magnetization of supercondcuting cuprate is shown as a function of temperature and clearly shows the transition to a superconducting state [6]. This is just one example of how a SQUID can be used to determine the transition temperature of a system into or out of a magnetic state. The same principle can be used to understand transitions as a function of magnetic field as well.

In order to better understand the spin structure of a system, a SQUID can be used to measure the magnetization as a function of magnetic field. In complex magnetic systems, determining the correct model to describe the underlying spin physics is often difficult. Magnetization measurements obtained via SQUID are vital for this process. In $Cr_{1/2}NbS_2$, for example, by comparing magnetization measurements to modeled results, it was shown that the intercalated Cr spins are described by a Heisenberg Spin Hamiltonian with an added interaction known as a Dyzaloshinkskii-Moriya interaction and

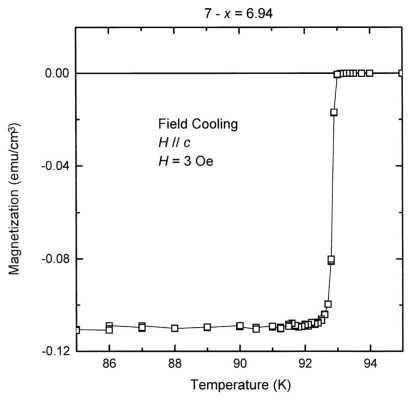

Fig. 7. The magnetization as a function of temperature for a superconducting sample of YBCO measured via a SQUID from reference [6]. The system undergoes a clear phase transition to a superconducting state at $T \approx 93K$.

crystaline anisotropy [7]. In this example, the magnetization was measured as function of magnetic field for three different field orientations as shown in figure 8. Again this is just one of many possible instances in which magnetization data can be compared to models to determine underlying spin physics. This is such a fundamental part of modern condensed matter physics that it is hard to find a material where this has not been done.

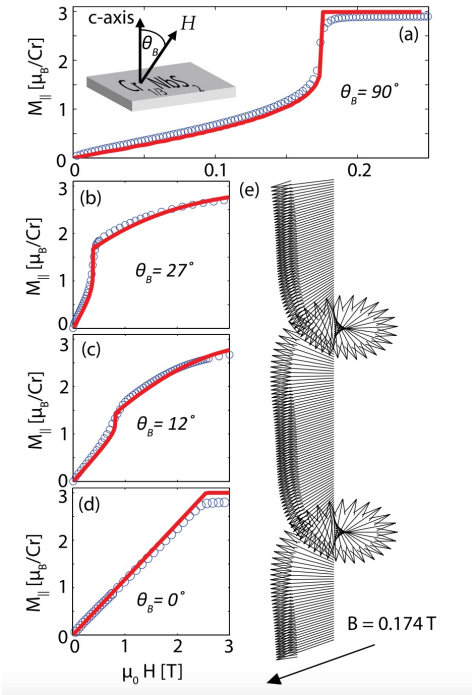

Fig. 8. (a-d) The magnetization of $Cr_{1/2}NbS_2$ as a function of magnetic field for four different field orientations from reference [7]. The red line is the modeled result from a Heisenberg Spin Hamiltonian with a Dyzaloshinkskii-Moriya interaction while the blue dots are the actual measured data. The units are represented such that it is the magnetic moment per Cr ion. (e) The spin structure of the Cr ions determined from this data at $B = 0.174\,T$

SQUIDs can also be combined with other novel experimental techniques such as scanning probe microscopy. In a scanning SQUID Microscope, for example, a DC squid is attached to the end of an SPM and scanned across a sample. This allows for the determination of the magnetic properties of a system as a function of position [8]. The limiting factor to the spatial resolution is the size of the SQUID itself and currently SQUID loops are constructed that are on the order of 100nm [8]. With these systems the magnetic structure at the surface of a material can be mapped with excellent resolution. These microscopes have been used to map out the edge currents in quantum wells for example [10]. Because currents generate a magnetic field, the currents in a material can be mapped out using a scanning SQUID microscope [8], [10]. This is especially useful as non-trivial topolical phases are investiagted in materials as some of these systems lead to edge currents [8]. They have also been used to determine spatial inhomogeneity of the superconducting phase in 2D Niobium doped $SrTiO_3$ [9]. Figure 9 shows this inhomogeneity at $330mK$ [9]. Similarly with figure 7, the lower magnetic flux is an indication that the sample is superconducting because of the Meissner effect. This inhomogeneity in the superconducting state is very useful for understanding the effects of local structural and doping variations [9].

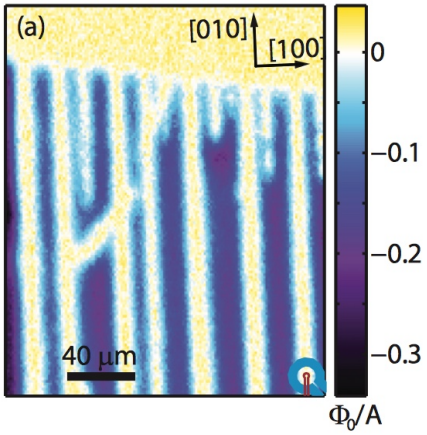

Fig. 9. The magnetization as a function of position in Niobium doped $SrTiO_3$ thin films as reported in reference [9]. Here a SQUID is scanned across the sample to determine the magnetic properties as a function of position.

Ultimately it is difficult to outline just how universal SQUIDs are in modern condensed matter physics. From basic crystal characterization to scanning SQUID microscopy, there are very few experiments that are not at least tangentially connected to the use of a SQUID.

IV. Conclusion

Because of this, the SQUID is one of the most versatile magnetic flux measurement techniques in modern physics. Here we have outlined the basic principles which govern the behavior of the DC and RF SQUID and given a very brief outline of the SQUID's myriad uses. To say that this treatment of the applications is complete would be a mischaracterization as

SQUIDs are relevant to everything from quantum computing to detectors at CERN.

V. Appendix

Here we will discuss the wave function (1) and its motivation as based on reference [3]. At temperatures near the phase transition T_C it can be derived directly from BCS theory, as was first done by Gor'kov in 1959 [2]. This means that this wavefunction is not explicitly valid for all temperatures, but is still applicable for the analysis here because it preserves the macroscopic physics we are dealing with.

To begin this analysis we turn to the cooper pair, a bound state of two electrons, one with spin up and one with spin down. The wave function for one cooper pair added to an inert Fermi See can be written as follows: [1]:

$$\Psi(\vec{\rho}) = e^{i\vec{q}\vec{R}} \cdot \sum_{\vec{k}>\vec{k_f}} A(\vec{k}) \cdot e^{i\vec{k}\vec{\rho}} \tag{11}$$

where $\vec{\rho} = \vec{r_1} - \vec{r_2}$, the center of mass coordinate is $\vec{R} = 1/2(\vec{r_1} + \vec{r_2})$ and the center of mass momentum is $\vec{q} = 1/2(\vec{k_1} + \vec{k_2})$ (which is zero here owing to the cooper pair being composed of two electrons with opposite momentum i.e. $\vec{k}$ and $-\vec{k}$). For simplicity we will only look at the spatial part of the wavefunction and not worry about the symmetry requirements.

We will be interested in the electrodynamics of this wavefunction so we can now consider the effects of an electric field, which will add a finite momentum $\hbar\vec{q}$ to the cooper pair.

We can also assume that the N particle wavefunction can be expressed as the product of all single cooper pair wavefunctions. Taking this analysis one step further, since cooper pairs are bosons they are not restricted by the Pauli exclusion principle. Therefore, we can imagine a state where all cooper pairs are condensed in the lowest energy state. Since the cooper pairs are in the same state any applied field will give all the cooper pairs the same momentum $\hbar\vec{q}$. Therefore the wave function (without antisymmetrisation) can be estimated as:

$$\Phi(\vec{R_1}, \vec{R_2}, ..., \vec{R_N}) = e^{i\vec{q}(\vec{R_1}+\cdots+\vec{R_N})}\Psi(\vec{\rho_1}) \cdots \Psi(\vec{\rho_N})$$

This state has a precisely defined phase at each point $\vec{r}$ in the superconductor if there is a large number of cooper pairs. Similarly, the wave functions for the relative coordinates can be thought of as a cooper pair density since they are functions of position. From this we can see where the wave function outlined in (1) is not completely unjustified and has a physical basis in the physics of cooper pairs. Clearly this is just an intuitive picture and not an rigorous derivation.

References

[1] Schrieffer, J. Theory Of Superconductivity Avalon Publishing, 1983

[2] Gorkov LP. Microscopic derivation of the Ginzburg-Landau equations in the theory of superconductivity. Sov. Phys. JETP. 1959 Jan 1;9(6):1364-7.

[3] Kopitzki, K.,Einfhrung in die Festkrperphysik, Springer Berlin Heidelberg, 2017

[4] Duzer T.V., Turner C.W., Principles of Superconductive Devices and Circuits, 1998

[5] Feynman, R. Leighton, R. Sands, M., The Feynman Lectures on Physics, Pearson/Addison-Wesley, 1963

[6] Ruixing Liang, D. A. Bonn, W. N. Hardy, Growth of high quality YBCO single crystals using BaZrO3 crucibles Physica C: Superconductivity Volume 304, Issues 1-2, 1 August 1998, Pages 105-111

[7] Benjamin J. Chapman, Alexander C. Bornstein, Nirmal J. Ghimire, David Mandrus, and Minhyea Lee, Spin structure of the anisotropic helimagnet Cr1?3NbS2 in a magnetic field Appl. Phys. Lett. 105, 072405 (2014)

[8] Kathryn Ann Moler, Imaging Quantum Materials, Imaging quantum materials, Nature Materials 16, 1049?1052 (2017)

[9] Hilary Noad, Eric M. Spanton, Katja C. Nowack, Hisashi Inoue, Minu Kim, Tyler A. Merz, Christopher Bell, Yasuyuki Hikita, Ruqing Xu, Wenjun Liu, Arturas Vailionis, Harold Y. Hwang, and Kathryn A. Moler Variation in superconducting transition temperature due to tetragonal domains in two-dimensionally doped SrTiO3 Phys. Rev. B 94, 174516 (2016)

[10] Eric M. Spanton, Katja C. Nowack, Lingjie Du, Gerard Sullivan, Rui-Rui Du, and Kathryn A. Moler Images of Edge Current in InAs/GaSb Quantum Wells Phys. Rev. Lett. 113, 026804 (2014)

[11] Magnetic Property Measurement System Hardware Reference Manual. Quantum Design, San Diego CA. http://mmrc.caltech.edu/MPMS/Manuals/QD